Hindawi Publishing Corporation
Journal of Control Science and Engineering
Volume 2013, Article ID 801237, 10 pages
http://dx.doi.org/10.1155/2013/801237

Research Article

Real-Time Energy Management Control for Hybrid Electric Powertrains

Mohamed Zaher and Sabri Cetinkunt

University of Illinois at Chicago, Chicago, IL 60607, USA

Correspondence should be addressed to Mohamed Zaher; mhzaher@asme.org

Received 19 December 2012; Accepted 9 April 2013

Academic Editor: Salem Haggag

This paper focuses on embedded control of a hybrid powertrain concepts for mobile vehicle applications. Optimal robust control approach is used to develop a real-time energy management strategy. The main idea is to store the normally wasted mechanical regenerative energy in energy storage devices for later usage. The regenerative energy recovery opportunity exists in any condition where the speed of motion is in the opposite direction to the applied force or torque. This is the case when the vehicle is braking, decelerating, the motion is driven by gravitational force, or load driven. There are three main concepts for energy storing devices in hybrid vehicles: electric, hydraulic, and mechanical (flywheel). The real-time control challenge is to balance the system power demands from the engine and the hybrid storage device, without depleting the energy storage device or stalling the engine in any work cycle. In the worst-case scenario, only the engine is used and the hybrid system is completely disabled. A rule-based control algorithm is developed and is tuned for different work cycles and could be linked to a gain scheduling algorithm. A gain scheduling algorithm identifies the cycle being performed by the work machine and its position via GPS and maps both of them to the gains.

1. Introduction

Fuel efficiency and reduced emissions are two of the most important considerations in all combustion-based power generation, including diesel engines [1]. In order to meet these demands, alternative powertrain concepts including all electric, hybrid, and fuel cell are being developed. The concept behind the hybrid devices is to store the otherwise wasted regenerative mechanical energy in energy storage devices and reuse that energy later in the work cycle. The regenerative energy recovery opportunity exists in every condition where the speed of motion is in opposite direction to the applied force or torque (Figure 1 [2]). This condition is satisfied in various conditions such as (Figure 2) the following:

(1) vehicle braking (i.e., slowdown to a lower speed on zero slope or vehicle is moving down a hill and braking must be applied to maintain a desired speed),

(2) load is moved by gravitational (load) force.

A parallel electric-hybrid powertrain concept is discussed in the next section. The real-time control challenge is to balance the machine power demands from both the engine and the hybrid storage device. The constraints faced in developing the control strategy are as follows:

(1) minimize fuel consumption while meeting low emission requirements,

(2) maintain or improve the work-machine productivity,

(3) prevent the depletion of the energy storage device, and maintain an acceptable state of charge (SOC).

A rule-based control strategy with multiple tunable gains for different work cycles is developed. The control algorithm should be robust and have low sensitivity to gain changes to accommodate real working conditions. This paper focuses on controlling hybrid powertrain mobile vehicles in real time via an optimal robust control that will enable continuous operation through repetitive and between different cycles. Yafu and Cheng [3] studied mild hybrid electric vehicles (HEV) with integrated starter generator (ISG). They used a parallel assist control strategy and modeled the system in Simulink and achieved their objective of reducing the fuel consumption.

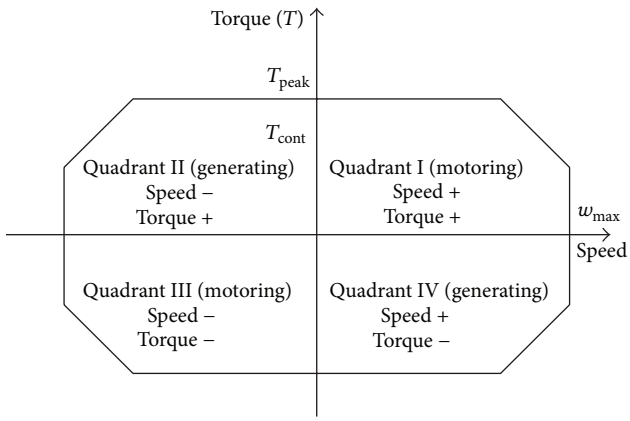

Figure 1: Torque versus speed motoring and generating quadrants (adopted from [2]).

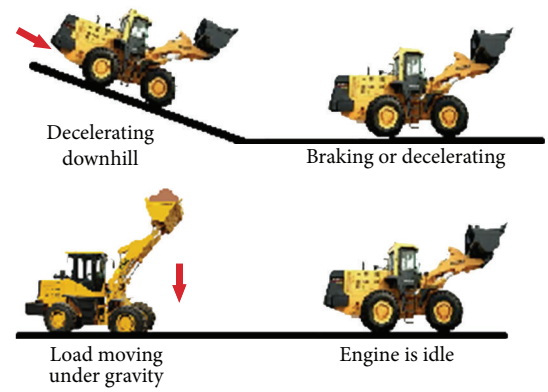

Figure 2: Regeneration opportunities.

Steinmaurer and del Re [4] used an ISG with an HEV with a statistics-based control to achieve task optimization in an attempt to emulate dynamic programming.

Two control algorithms are most commonly investigated in the literature [1]. Kessels et al. [5] surveyed the control algorithms for HEVs up to 2007. Liu and Peng [6] studied the control of Toyota PSHEV using two control algorithms: stochastic dynamic programming and equivalent consumptions minimization strategies (ECMS) [7]. They concluded that, with ECMS, frequent shifting should be avoided by adding extra constraints between gear switching decisions, while with stochastic dynamic programming approach (SDP) an extra input operating gear mode is needed beside the engine speed and the SOC. Syed et al. [8] used a fuzzy logic gain scheduling algorithm with proportional-integral (PI) controllers which are used with power-split HEV (PSHEV). The results of testing the controller on a Ford Escape showed that a minimum of four rules are needed to ensure smooth engine speed. Canova et al. [9] studied the engine start/stop dynamics, which led to an engine model that is used in a linear quadratic regulator control algorithm. Lin et al. [10] studied the dynamics of the Toyota Prius PHEV and developed an optimal control energy management strategy and artificial neural networks, that was modified to a suboptimal controller.

Gokasan et al. [11] used sliding mode control to limit the series HEVs to the optimal efficiency operating range and compared it to PI controllers. They used two simultaneous sliding mode controllers one to control the engine speed, and the other to control the engine torque. Moura et al. [12] used SDP in PHEV power management and explored the potential of charge depletion, overcharging, and the economy of fuel-electric usage in hybrid technology. Their approach allows for energy management control without prior knowledge of the driving cycle. Johannesson et al. [13] developed a GPS-based SDP control algorithm for HEV that utilizes the travel and location information of the HEV to manage its power sources to assess the potential benefit of predictive controls. They compared a position-dependent controller and a position-invariant one to an optimal control algorithm which showed a slight reduction in fuel consumption when the position information is taken into account. However, they also discovered that only the average travel information is needed and the high level of detail of travel conditions is not needed.

Huang et al. [14] used a threshold logic control strategy that is optimized continuously during operation to control a PHEV. Lee et al. [15] developed neuro-fuzzy technique to analyze and learn GPS data and control the hybrid vehicle to improve fuel economy and reduce emissions. Fu [16] developed a methodology for real-time prediction of torque availability in interior permanent magnet motors. When implemented on HEVs, it prevents torque requests at times when there are no availabilities, hence protecting the battery from depletion. According to Borhan et al. [17] dynamic programming requires knowledge of the upcoming cycle while ECMS are less sensitive to computation, short-sighted, and sensitive to their parameters. Borhan et al. [17] linearized the models and simulated over different driving cycles. They modeled the system using the resistance torque, rate of SOC equations, and Willan's line method. For this reason, MPC strategy for PSHEV has been developed to minimize fuel consumption, reduce service brake usage, and prevent overcharge and discharge of the battery. Hybrid powertrain technology has been studied and implemented in passenger vehicles and trucks; yet very little literature can be found about hybrids in construction equipment applications. Grammatico et al. [18] implemented PSHEV technology in small wheel loaders and used a classic proportional-integral-derivative controller (PID) to control the system.

The machine investigated in this work is a medium wheel loader (MWL). However, the procedures used are general such that they are applicable to other types of work machines.

2. Medium Wheel Loaders and Hybrid Technology

The prototype machine selected is a medium wheel loader (MWL). A detailed dynamic machine model is described in Figure 3. For this purpose, accurate virtual models with relatively high fidelity are needed to attempt mimicking the actual machine. However, replicating every aspect of the

machine in virtual reality is impossible due to difficulties in modeling actual physics. A detailed virtual dynamic machine model is developed using the mathematical equation and embedded in S-functions in Simulink. The model is that is validated by comparing it to experimental data. There are four general work cycles for this type of machine: truck-loading, load-and-carry, pile dressing, and roading. Both the truck-loading and the load-and-carry are cycles that involve digging, moving earth from one location to another and dumping it at the new location. The truck-loading is loading a truck or a hopper with earth and is categorized into two major cycles: aggressive truck-loading (ATL) and moderate truck-loading (MTL). ATL is characterized by its speed and the machine is operated with the engine at full throttle at all times.

Moderate truck-loading (MTL) can be as fast as or slower than ATL but the operator varies engine speed command and may never reach full throttle. The load-and-carry cycle is moving dirt to a hopper far away from the pile and is defined by the travel distance into short and long. Pile dressing is moving the earth in the pile around to make it ready for the following operations. Roading is driving the loader from one location to another without being involved in any of load movements. There are five main systems in loaders, namely,

(1) engine,

(2) transmission and lower powertrain,

(3) hydraulics (for work tool and steering),

(4) controllers, and

(5) chassis (frame cabin and linkages).

The engine is the primary source of energy for this machine from which all power requirements are drawn. The torque provided by the engine is split between two, the powertrains which are responsible for the motion of the loader and the hydraulics which are responsible for mainly linkages operations and possibly braking, cooling fan motoring, and steering.

2.1. Engine. The engine is a four-stroke turbocharged after cooled injection approximately 9-liter diesel engine, with average power rating (Figure 4) of 224–261 kW at 1800–2200 rpm and compression ratio of 17 : 1. The output gross power from the engine is not the actual available power to the wheel loader main systems due to the power consumptions from accessories such as the alternator, the muffler, the emission control, and the cooling system [19]. Thus, the power losses in the range of 6–14% must be considered when calculating the net available power to the powertrain and the hydraulics. Unlike automotive engines, the diesel engine speed in construction equipment applications is limited to about 2300 rpm. This is due to the need for higher torque values at lower machine speeds, the desire for longer engine life and reduced fuel consumption. The engine dynamic model allows for the calculation of the torque and speed along the lug curve and calculating the engine fuel consumption via the brake fuel consumption map. With hybrid implementation this engine is downsized to approximately 7 liters of diesel allowing the engine to run in a more efficient zone and making the hybrid system more cost effective.

Table 1: Transmission ratios.

Gear shift	Gear ratio
4F	−0.77
3F	−1.36
2F	−2.44
1F	−4.66
N	0
1R	4.22
2R	2.21
3R	1.23
4R	0.70

2.2. Transmission and Lower Powertrain. The main function of the powertrain is to transfer the power from the engine to the wheels in order to create the necessary rimpull for the motion through a series of speed reductions and torque multiplications. The powertrain of a wheel loader consists of wheels, axle reductions, differentials, axles, a torque converter (TC), and transmission (Figure 5 (http://www.caranddriver.com/photos-09q4/309587/2010-bmw-activehybrid-x6-automatic-transmission-and-electric-motor-diagram-photo-310275)).

A TC is a hydrodynamic coupling device which transfers power between its input and output while absorbing the difference in speed between the two shafts by slipping. The difference in power between input and output is absorbed and dissipated in the oil inside the TC in the form of heat. The two main defining characteristics of the TC are the primary torque T_p which is the value of the rated torque of the impeller at the rated speed N_{rated} (usually 1700 rpm) and the torque ratio T_r which is the ratio between the output turbine torque and the input impeller torque. Also, T_r is function of the speed ratio S_r which is the ratio between the output turbine speed and the input impeller speed (N_i). Through the knowledge of T_p, S_r, and the rated and the input speed N_i and the input torque T_i can be calculated at various speeds using (1) and Figure 6:

$$T_i = T_p\big|_{S_r}\left(\frac{N_i}{N_{\text{rated}}}\right)^2. \quad (1)$$

The TC is followed by a planetary gearbox which reduces the output speed to a desired range for the machine ground velocity. The gearbox is constituted of several planetary gear trains connected together via electrohydraulically controlled brakes and clutches which are used to select the gear. The explanation of how the mechanism works is available in the literature [19]. The regular gear train in wheel loaders has four forward speeds, four reverse, and one neutral (Table 1). The dynamic transmission model is based on multiple look-up tables for the gear combinations and clutches' pressures.

2.3. Hydraulics. The hydraulic system of the prototype MWL machine used in this study is a closed center load sensing

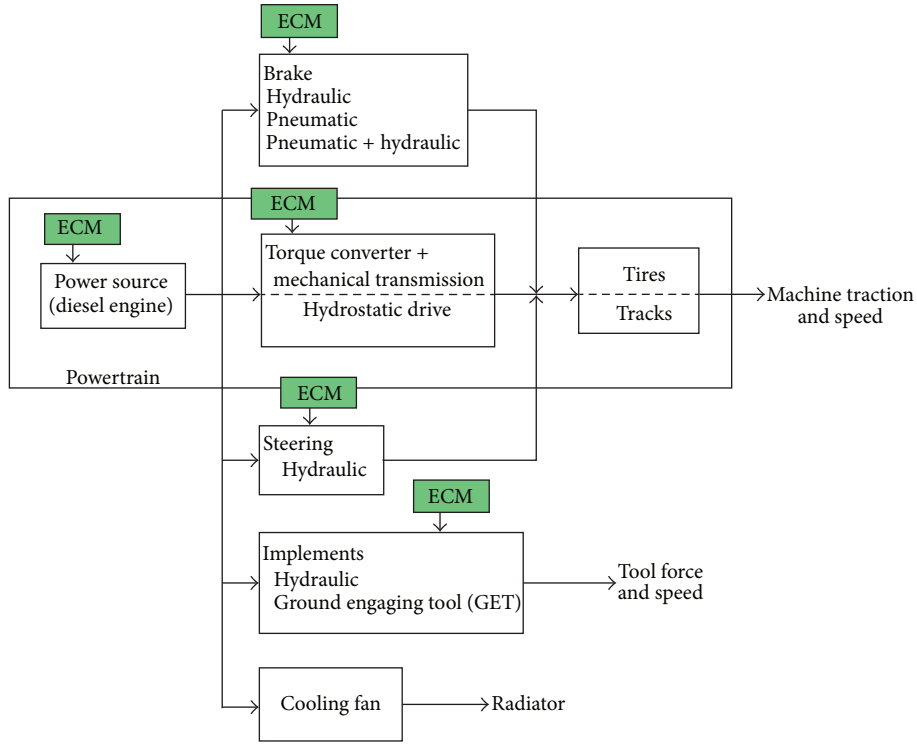

Figure 3: Wheel loader systems.

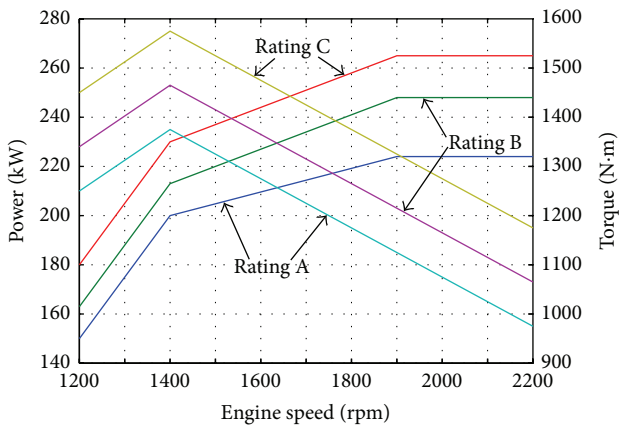

Figure 4: Rated engine lug curve and power rating.

hydraulics system for the work tool (implement) circuit. This system is the common trend in MWL as it avoids dissipation of energy and adapts the amount of flow provided by the pump to meet the needs of the machine, thus minimizing the losses unlike open center systems. The load sensing system compares the pump pressure at the output to the cylinders pressures, and then it adjusts the pump's swash plate based on that feedback in order to maintain a certain pressure differential (Figure 7 (http://www.mobilehydraulictips.com/efficient-mobile-hydraulic-systems/)). A shuttle valve senses the highest pressure between the tilt and lift pressures and sends it through feedback for comparison. Equation (2) governs the angle of the pump's swash plate [2]:

$$\theta_{\text{cmd}} = \theta_{\text{offset}} + K\left(\Delta P_{\text{cmd}} - \left(P_s - P_L\right)\right), \tag{2}$$

where θ_{cmd} is the commanded swash plate angle, θ_{offset} is the swash plate angle offset from the desired position, K is a gain, ΔP_{cmd} is the desired pressure differential, P_s is the pump outlet pressure, and P_L is the load pressure.

A pressure limiting control system in the pump is called the high pressure cut-off or pressure compensator, whose function is to limit the maximum system pressure by reducing pump displacement to zero when the set pressure is reached. The post compensation regulates the amount of flow sent to the tilt and lift based on the pressure feedback from both valves such that the valve with the higher pressure receives more flow than that with the lower pressure; that is, it maintains a constant pressure drop across the valve. The spool movement of a compensator valve is governed by (3):

$$\Delta x_s = \frac{1}{K_{\text{spring}}}\left(p_s A_s - p_l A_l\right), \tag{3}$$

where p_s is the supply pressure, A_s is the area of the piston at the supply pressure side, p_l is the load pressure, A_l is the area of the piston at the load pressure side, K_{spring} is the spring coefficient, and Δx_s is the length of the opening from the supply to the load in the valve. Equations (4) through (7)

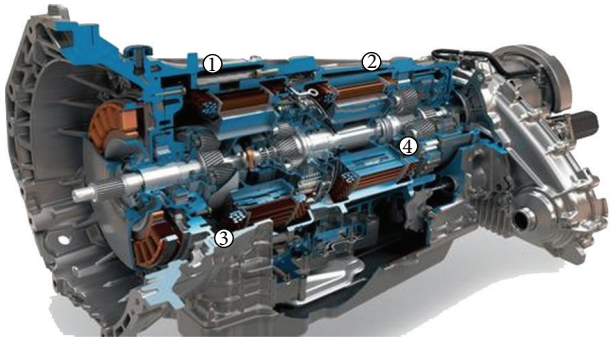

Figure 5: Transmission.

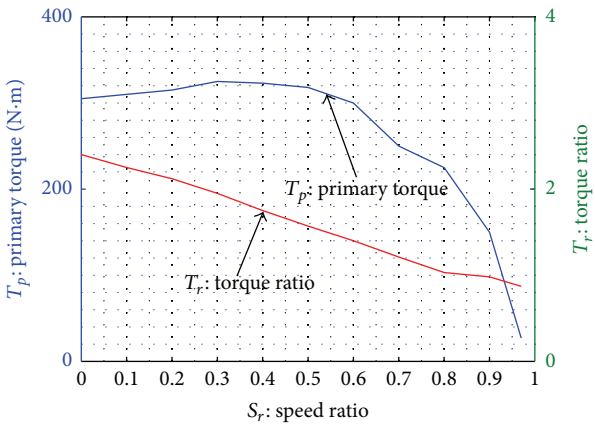

Figure 6: Torque converter characteristics.

govern the dynamics and static hydraulics and the hydromechanical equations,

$$Q = \frac{V\dot{P}}{\beta}, \tag{4}$$

$$Q = C_d A \sqrt{\frac{2\Delta P}{\rho}}, \tag{5}$$

$$Q = A\dot{x}, \tag{6}$$

$$F = PA, \tag{7}$$

where β is the bulk modulus, Q is the volumetric flow rate, P is the pressure, ρ is the oil density, C_d is the valve coefficient, A is the valve opening area, and x is the displacement of the piston.

2.4. Chassis. The chassis is the body and linkages of the machine and it is governed by the mechanical kinematic constraints and dynamics which can be represented using multibody dynamics approaches.

2.5. Electric Hybrid. The electric hybrid concept (Figure 8) is used to convert the regenerative mechanical energy to electrical energy via an electric generator and then store it in electrochemical batteries. The electric hybrid consists of a dual-function motor/generator (ISG) actuator, an inverter that requires a separate cooling system, and a lithium-Ion battery pack. The Li-I battery was selected as it is the most promising rechargeable battery technology available and is widely used in electric hybrid technology [20]. The SOC changes over time interval dt, with discharging or charging current i. The battery SOC can be calculated using (8):

$$\mathrm{SOC} = \mathrm{SOC}_0 - \int \frac{i(t)}{Q(i(t))} dt, \tag{8}$$

where $Q(i(t))$ is the ampere-hour capacity of the battery at current rate $i(t)$. While the electric hybrid is the most expensive, it is receiving the most investment in all mobile industries due to its maturity. With the engine downsizing, the ISG system costs come to neutral. The diesel engine is the primary power plant; electric hybrid is the energy bumper. The ISG adds power to powertrain from the battery when power assist is needed. It also stores the energy to the battery from the powertrain when a power storage opportunity exists. The electric hybrid cooling cycle passes through all the components where the coolant fluid goes through the shunt tank into radiator, through the pump, inverter, battery, and ISG and then back to radiator. Also, the shunt tank is connected to all the hybrid parts to allow air bubbles to escape and to the radiator to allow coolant to expand and supply excess fluid.

3. Control Strategies

In this section, the proposed control strategy is presented. The control strategy under investigation is a rule-based control. Based on the analysis and the results it will be determined if gain scheduling via GPS tracking and cycle recognition algorithm is needed. The rule-based control gains are tuned to different cycles to minimize the fuel consumption, bring the final SOC closest to the initial SOC, minimize the cycle time, and regulate the minimum engine speed to be close to 1000 rpm or higher (Figure 9). The high-level Simulink diagram is shown (Figure 10).

3.1. Cycle Model. The cycle model is built to mimic the commands of the real operator sent to the different machine systems, as well as the work area. In total, there are four different cycles and hence four different operator models used in this investigation: ATL, MTL, short load-and-carry (SLC), and long load-and-carry (LLC). Table 2 shows the input and output signals to the operator model. The cycle model is modeled as "if statements" with multiple possible output scenarios based on time and distance along the cycle. Each if statement output corresponds to a group of time- and distance-based operator commands to the machine. The sequence of these commands will result in the machine operations that will lead to completing the cycle. Table 3 shows the input and output signals to the controller.

3.2. Rule-Based Logic. The rule-based control (Figure 10) is designed based on knowledge of machine functions and system of the machine. This control is torque-based control

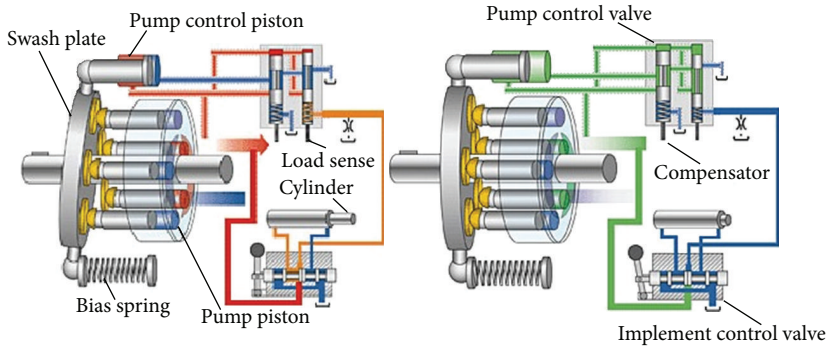

Figure 7: Load sensing axial piston pump with swash plate (http://www.mobilehydraulictips.com/efficient-mobile-hydraulic-systems/).

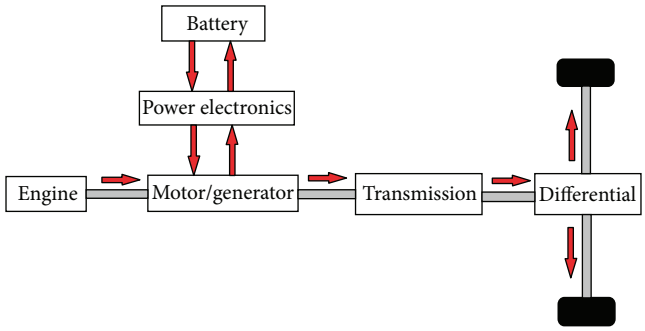

Figure 8: Electric hybrid concept (adopted from [6]).

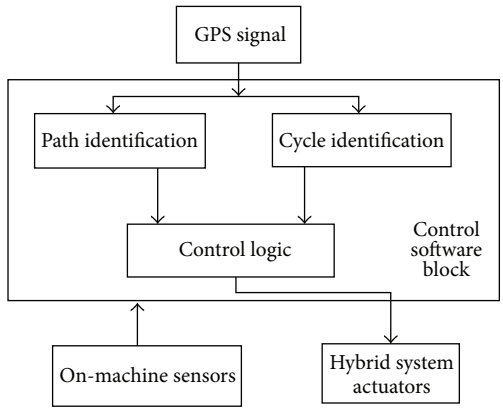

Figure 9: Rule-based control block diagram.

Table 2: Operator model signals.

Cycle model input signals	Cycle model output signals
(1) Engine speed (rpm)	(1) Desired engine speed (rpm)
(2) Desired gear number	(2) Gear command
(3) Lift displacement (m)	(3) Lift command
(4) Tilt displacement (m)	(4) Tilt command
(5) Machine ground velocity (m/s)	(5) Brake command
	(6) Bucket load
	(7) Grade
	(8) Drawbar

Table 3: Rule-based logic signals.

Input signals	Output signals
(1) Engine speed (rpm)	(1) ISG torque command
(2) Desired engine speed (rpm)	
(3) Engine load torque (Nm)	
(4) Engine maximum torque (Nm)	
(5) SOC	
(6) Gear command	
(7) Grade	

that will send out desired torque to the ISG and based on this the generator-motor action will be determined. To decide whether to charge or assist multiple factors are considered. These factors are represented by gains and thresholds that will enable reaching the decision. These gains and thresholds are tuned for different cycles to achieve optimum robust results based on the criteria listed earlier. The gains tuned in this logic are: delay timer, assist threshold, charge threshold, low SOC threshold, idle charge torque, ISG torque-required threshold, engine speed factor, assist/charge threshold offset, and the idle charge SOC threshold.

To reach this decision, the first step is to multiply the engine torque limit by three of the gains and compare the results to the engine load torque. These gains are the assist threshold, charge threshold, and hysteresis factor. Another gain existing to assist in decision making is the low SOC threshold which is biased to charging when the SOC drops below it. For low SOC mode, the more aggressive (charge bias) assist/charge thresholds should be arrived at by taking the standard values and offsetting them by assist/charge threshold offset. Along with comparison of the engine speed and torque demand with the actual, this procedure will determine the torque demand out of the engine. This step determines if the engine is capable of supplying the demanded power on its own, needs assistance from the hybrid, or has excess power to be used for charging. If the engine is idle and the SOC is less than the idle SOC charge

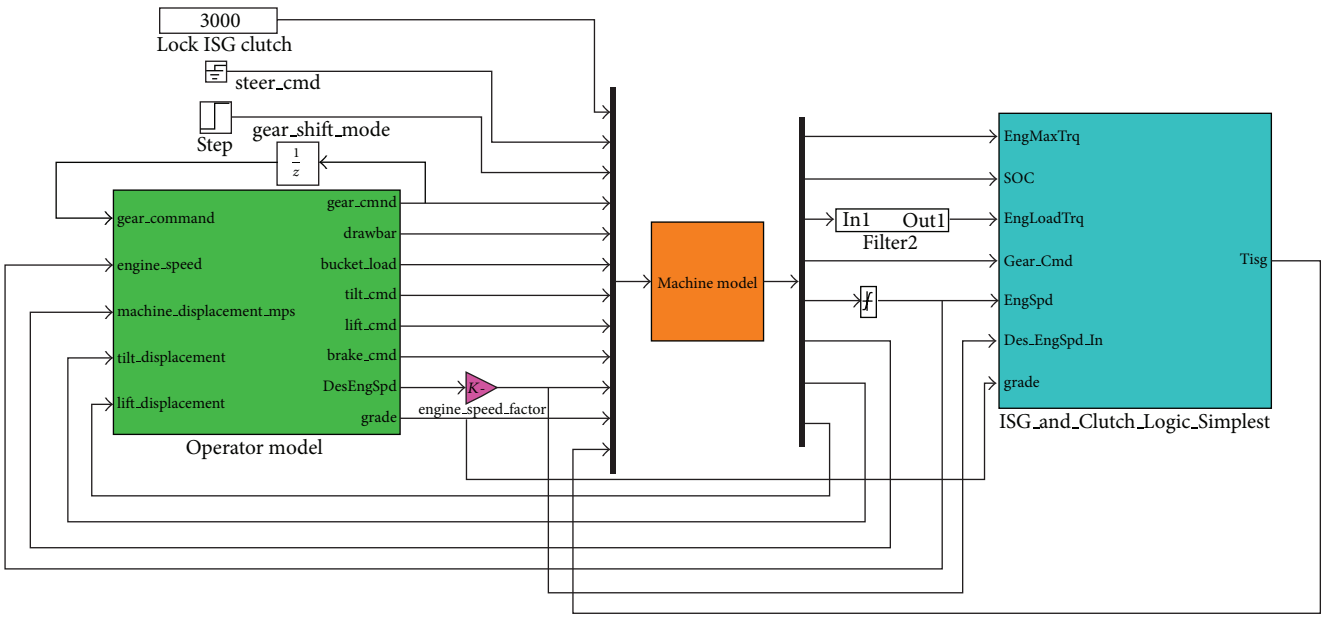

Figure 10: Rule–based control upper level Simulink diagram.

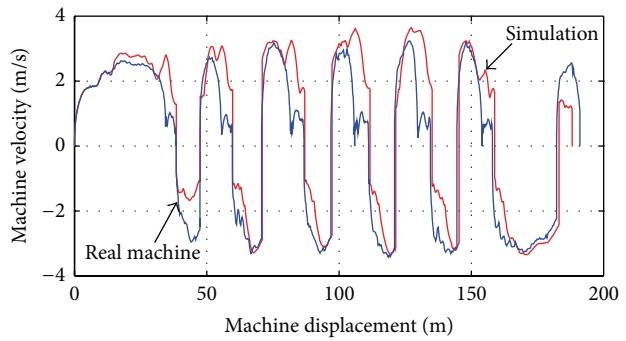

Figure 11: Validation machine velocity.

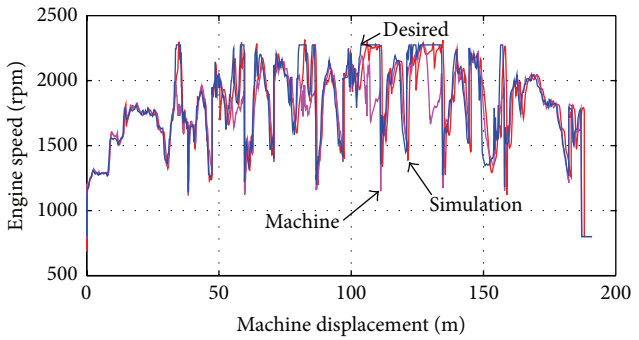

Figure 12: Validation engine speed.

threshold, then a charge command is issued. Charging is also enforced when the retard engine speed threshold is exceeded.

With any gear upshift or if the engine deceleration rate exceeds the engine deceleration rate threshold, assist is triggered. The gain tuning process is an iterative and time-consuming process. The objective is to obtain an optimal set of parameters for robust design such that slight changes in the gain values do not affect the performance much. The orthogonal array experiments only require a fraction of the full-factorial combinations and the same result can be achieved. This can be done by using the analysis of the variance (ANOVA) thus making it the most suitable for tuning the nine gains. A predictive model based on the ANOM is then formulated through which an estimate of the optimal set of interactions is determined and tested. By repeating this process over time, the desired optimal robust solution can be obtained for each cycle [21].

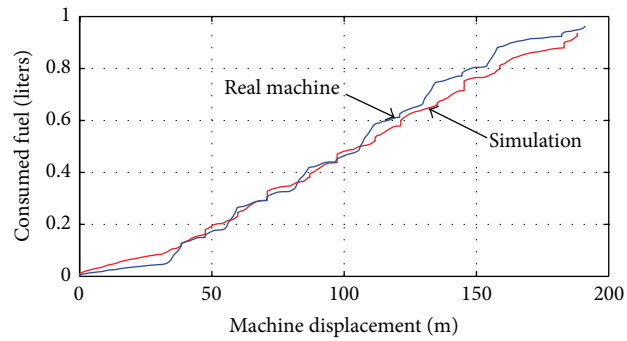

Figure 13: Validation consumed fuel.

4. Results

In this section, the machine virtual dynamic model validation as well as the results obtained during this work is presented. The validation results show that the used machine model is in good correlation with the real-life machine. The results

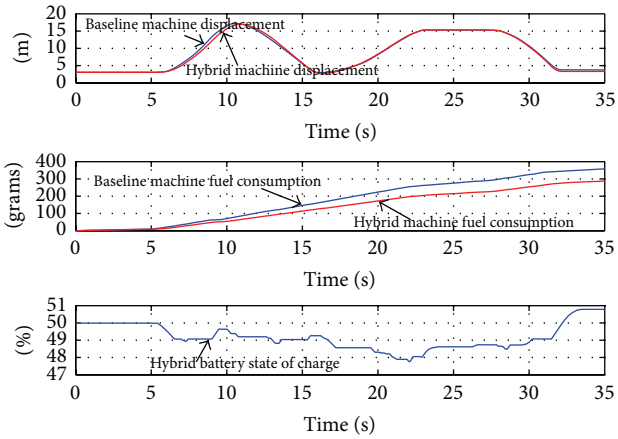

Figure 14: ATL hybrid versus baseline.

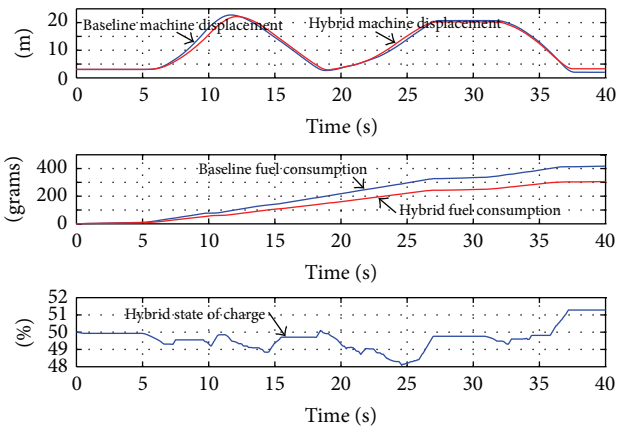

Figure 15: Moderate truck loading cycle.

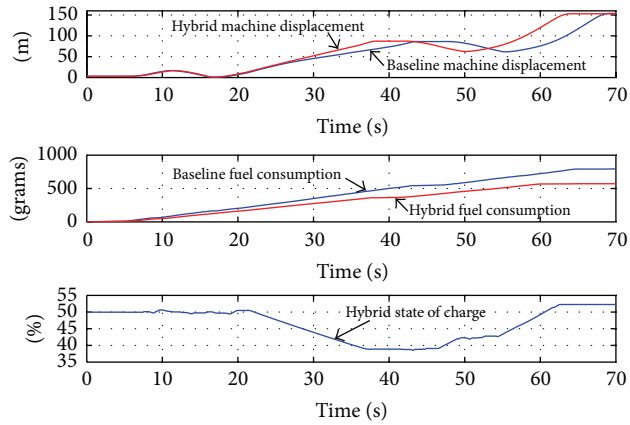

Figure 16: Short load and carry cycle.

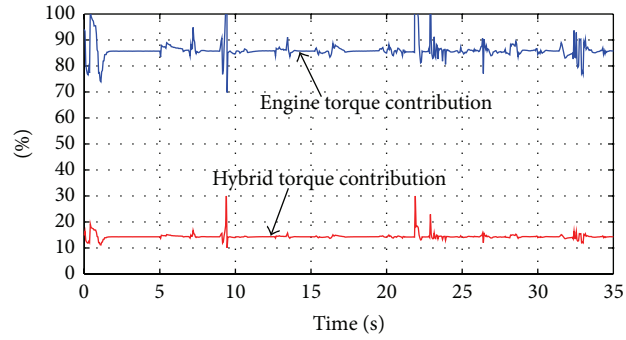

Figure 17: Torque contribution.

obtained show that when the engine is downsized, the hybrid system is implemented, its control logic gains are optimized, and the system performs very well without GPS or cycle recognition algorithm. The model validation is performed by obtaining machine data from the real-life wheel loader and giving the same operator commands to the machine model.

Figure 11 shows both the real and simulated machine velocities. The general speed pattern is the same and is in good agreement. The differences could be attributed to the use of approximate dynamics in the different machine systems. Figure 12 shows the desired engine speed sent by the operator to the machine and implemented in the cycle model, the real machine engine speed, and the simulated engine speed. From Figure 12 it is clear that the modeled engine speed response to the desired engine speed command matches to a great extend the actual engine speed response. The differences could be attributed to the use of approximation and estimated numbers in various points in the model including the load on the machine. Figure 13 shows the amount of fuel consumed by the machine versus that estimated by the machine model. The general trend of the fuel consumption is the same and the difference in the end point is minimal. Thus, it can be concluded that the machine model has a very good correlation with the real machine. Three work cycles were used in the analysis: ATL, MTL, and SLC cycles. Figure 14 compares between the baseline regular and the optimized hybrid wheel loader for the ATL cycle.

It is shown that maintaining productivity while decreasing the fuel consumption by 20% can be achieved by switching to the downsized hybrid machine. Figure 15 compares between the baseline regular and the optimized hybrid wheel loader for the MTL cycle. From the obtained results it is shown that maintaining productivity while decreasing the fuel consumption by 26.5% can be achieved by switching to the downsized hybrid machine.

Figure 16 compares between the baseline regular and the optimized hybrid wheel loader for the SLC cycle. From the obtained results it is shown that increasing productivity by 7.7% and decreasing the fuel consumption by 28% can be achieved by switching to the downsized hybrid machine. From Figure 17, it can be deduced that the hybrid system contributes to about 14–17% of the total torque needed by the machine. After the optimization of the control parameters for each independent cycle, the investigation of the effect of using these parameters in different cycles should be carried out. This investigation will determine if online cycle identification and GPS mapping of the worksite is needed.

The optimized gain of the MTL and SLC will be tested in the ATL and compared to the results obtained by its

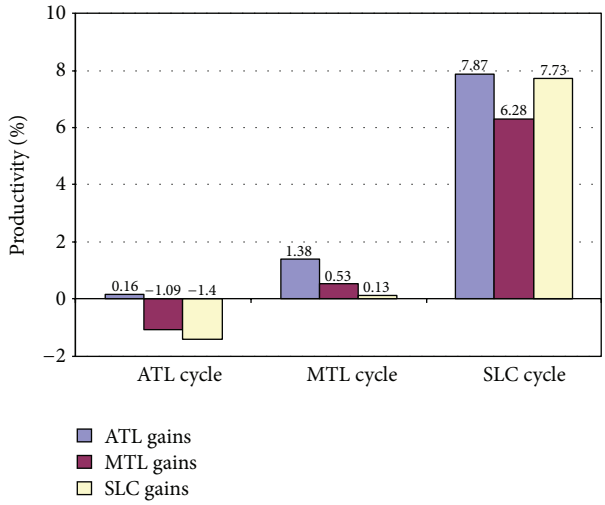

Figure 18: Effect of different gain groups on cycles' productivity.

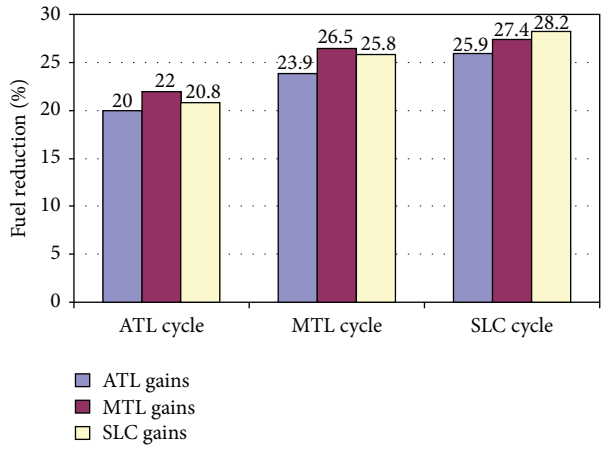

Figure 19: Effect of different gain groups on cycles' fuel reduction.

optimized gains, the gain groups of the ATL and SLC will be tested in the MTL and compared to the results obtained by its optimized gains, and the gain groups of the ATL and MTL will be tested in the SLC and compared to the results obtained by its optimized gains. By examining the results closely (Figures 18 and 19), all the cycles exhibit a change of less than 2% in terms of productivity and less than 3% in terms of fuel reduction from that of the optimized cycle.

From this it can be concluded that the knowledge of the running cycle is not needed as long as the machine is using any optimized set of parameters. Hence, online cycle identification and GPS mapping is not needed to be implemented on the machine but remains useful as an analysis tool for the worksite and operator performance.

5. Conclusions

The implementation of an electric hybrid powertrain on a medium wheel loader is expected to maintain the productivity of the machine within acceptable range. The usage of the hybrid system with a downsized engine is expected to reduce the fuel consumption on the machine by 20–30% at different cycles. The hybrid system supplies 14–17% of the torque required by the machine during its work cycle. By optimizing the hybrid controller gains for any work cycle, the controller can be used with any work cycle. Thus, the GPS tracking and gain scheduling algorithms are not needed.

Abbreviations

ANOVA: Analysis of the variance
ATL: Aggressive truck-loading
BSFC: Brake-specific fuel consumption
CVT: Continuously variable transmission
ECMS: Equivalent consumptions minimization strategies
GPS: Global positioning system
HEV: Hybrid electric vehicle
ISG: Integrated starter generator
LLC: Long load-and-carry
MTL: Moderate truck-loading
MWL: Medium wheel loader
PHEV: Plug-in hybrid electric vehicle
PSHEV: Power-split hybrid electric vehicle
SDP: Stochastic dynamic programming
SLC: Short load-and-carry
SOC: State of charge
TC: Torque converter.

References

[1] C. D. Rakopoulos and E. G. Giakoumis, *Diesel Engine Transient Operation: Principles of Operation and Simulation Analysis*, Springer, 2009.

[2] S. Cetinkunt, *Mechatronics*, John Wiley and Sons, 2007.

[3] Z. Yafu and C. Cheng, "Study on the powertrain for ISG mild hybrid electric vehicle," in *Proceedings of the IEEE Vehicle Power and Propulsion Conference (VPPC '08)*, September 2008.

[4] G. Steinmaurer and L. del Re, "Optimal energy management for mild hybrid operations of vehicle with an integrated starter generator," SAE Technical Paper 2005-01-0280, pp. 73–80, 2005.

[5] J. T. B. Kessels A, J. Sijs, R. M. Hermans, A. A. H. Damen, and P. P. J. van den Bosch, "On-line identification of vehicle fuel consumption for energy and emission management: an LTP system analysis," in *Proceedings of the American Control Conference (ACC '08)*, Seattle, Wash, USA, June 2008.

[6] J. Liu and H. Peng, "Modeling and control of a power-split hybrid vehicle," *IEEE Transactions on Control Systems Technology*, vol. 16, no. 6, pp. 1242–1251, 2008.

[7] G. Paganelli, Y. Guezennec, and G. Rizzoni, "Optimizing control strategy for hybrid fuel cell vehicle," SAE Technical Paper 2002-01-0102, SAE, Warrendale, Pa, USA, 2002.

[8] F. U. Syed, M. L. Kuang, M. Smith, S. Okubo, and H. Ying, "Fuzzy gain-scheduling proportional-integral control for improving engine power and speed behavior in a hybrid electric vehicle," *IEEE Transactions on Vehicular Technology*, vol. 58, no. 1, pp. 69–84, 2009.

[9] M. Canova, Y. Guezennec, and S. Yurkovich, "On the control of engine start/stop dynamics in a hybrid electric vehicle," *Journal*

of Dynamic Systems, Measurement and Control, Transactions of the ASME, vol. 131, no. 6, pp. 1–12, 2009.

[10] X. Lin, H. Banvait, S. Anwar, and C. Yaobin, "Optimal energy management for a plug-in hybrid electric vehicle: real-time controller," in *Proceedings of the American Control Conference (ACC '10)*, pp. 5037–5042, Baltimore, Md, USA, July 2010.

[11] M. Gokasan, S. Bogosyan, and D. J. Goering, "Sliding mode based powertrain control for efficiency improvement in series hybrid-electric vehicles," *IEEE Transactions on Power Electronics*, vol. 21, no. 3, pp. 779–790, 2006.

[12] S. J. Moura, H. K. Fathy, D. S. Callaway, and J. L. Stein, "A stochastic optimal control approach for power management in plug-in hybrid electric vehicles," *IEEE Transactions on Control Systems Technology*, vol. 19, no. 3, pp. 545–555, 2011.

[13] L. Johannesson, M. Åsbogård, and B. Egardt, "Assessing the potential of predictive control for hybrid vehicle powertrains using stochastic dynamic programming," *IEEE Transactions on Intelligent Transportation Systems*, vol. 8, no. 1, pp. 71–83, 2007.

[14] Y. J. Huang, C. L. Yin, and J. W. Zhang, "Design of an energy management strategy for parallel hybrid electric vehicles using a logic threshold and instantaneous optimization method," *International Journal of Automotive Technology*, vol. 10, no. 4, pp. 513–521, 2009.

[15] S. H. Lee, S. D. Walters, and R. J. Howlett, "Intelligent GPS-based vehicle control for improved fuel consumption and reduced emissions," in *Proceedings of the 12th International Conference on Knowledge-Based Intelligent Information and Engineering Systems*, pp. 701–708, Zagreb, Croatia, 2008.

[16] Z. X. Fu, "Real-time prediction of torque availability of an ipm synchronous machine drive for hybrid electric vehicles," in *Proceedings of the IEEE International Conference on Electric Machines and Drives*, pp. 199–206, San Antonio, Tex, USA, May 2005.

[17] H. A. Borhan, A. Vahidi, A. M. Phillips, M. L. Kuang, and I. V. Kolmanovsky, "Predictive energy management of a power-split hybrid electric vehicle," in *Proceedings of the American Control Conference (ACC '09)*, pp. 3970–3976, June 2009.

[18] S. Grammatico, A. Balluchi, and E. Cosoli, "A series-parallel hybrid electric powertrain for industrial vehicles," in *Proceedings of the IEEE Vehicle Power and Propulsion Conference (VPPC '10)*, pp. 1–6, September 2010.

[19] F. Croce, *Optimal Design of Powertrain and Hydraulic Implement Systems for Construction Equipment Applications [Ph.D. thesis]*, University of Illinois at Chicago, 2010.

[20] M. Ehsani, Y. Gao, and A. Emadi, *Modern Electric, Hybrid Electric, and Fuel Cell Vehicles: Fundamentals, Theory, and Design Second Edition*, Taylor & Francis, 2010.

[21] Y. W. Fowlkes and C. M. Creveling, *Engineering Methods For Robust Product Design Using Taguchi Methods in Technology and Product Development*, Prentice Hall, 1995.

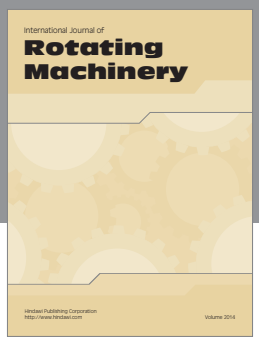

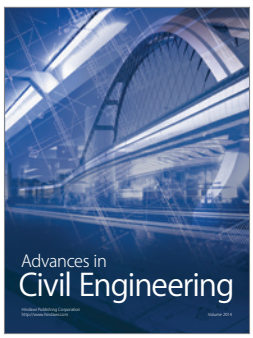

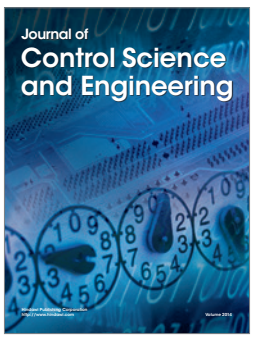

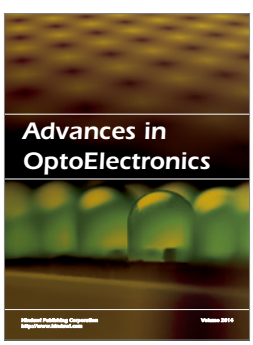

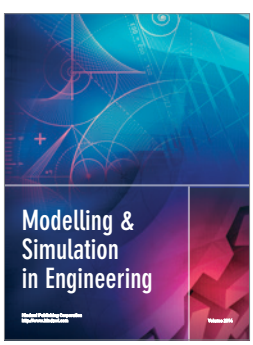

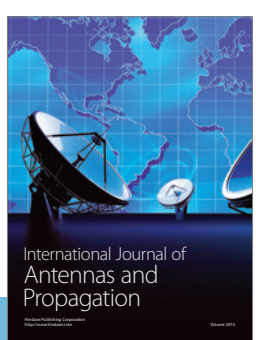

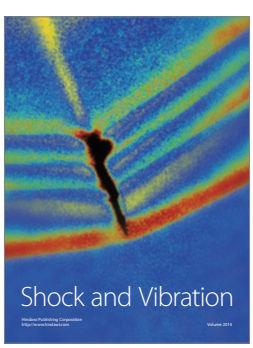

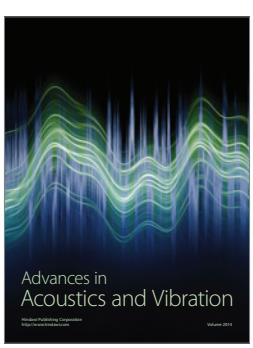

Hindawi

Submit your manuscripts at
http://www.hindawi.com